

---

# Consistent Collaborative Filtering via Tensor Decomposition

---

Shiwen Zhao<sup>1</sup> Charles Crissman<sup>1</sup> Guillermo R Sapiro<sup>1</sup>

## Abstract

Collaborative filtering is the *de facto* standard for analyzing users' activities and building recommendation systems for items. In this work we develop *Sliced Anti-symmetric Decomposition* (SAD), a new model for collaborative filtering based on implicit feedback. In contrast to traditional techniques where a latent representation of users (user vectors) and items (item vectors) are estimated, SAD introduces one additional latent vector to each item, using a novel three-way tensor view of user-item interactions. This new vector extends user-item preferences calculated by standard dot products to general inner products, producing interactions between items when evaluating their relative preferences. SAD reduces to state-of-the-art (SOTA) collaborative filtering models when the vector collapses to 1, while in this paper we allow its value to be estimated from data. The proposed SAD model is simple, resulting in an efficient group stochastic gradient descent (SGD) algorithm. We demonstrate the efficiency of SAD in both simulated and real world datasets containing over  $1M$  user-item interactions. By comparing SAD with seven alternative SOTA collaborative filtering models, we show that SAD is able to more consistently estimate personalized preferences.

## 1. Introduction

Understanding preferences based on users' historical activities is key for personalized recommendation. This is particularly challenging when explicit ratings on many items are not available. In this scenario, historical activities are typically viewed as binary, representing whether a user has interacted with an item or not. Users' preferences must be inferred from such *implicit* feedback with additional assumptions based on this binary data.

One common assumption is to view non-interacted items as

---

<sup>1</sup>Apple. Correspondence to: Shiwen Zhao <swzhao@apple.com>.

negatives, meaning users are not interested in them; items that have been interacted are often assumed to be preferred ones (Hu et al., 2008; Pan et al., 2008). In reality however, such an assumption is rarely met. For example, lack of interaction between a user and an item might simply be the result of lack of exposure. It is therefore more natural to assume that non-interacted items are a combination of the ones that users do not like and the ones that users are not aware of.

Rendle et al. (2009) pioneered the work of treating the non-interacted items as such a mixture and proposed a weaker assumption by giving partial orders between items. Particularly, they assumed that items which users have interacted with are more preferable than the non-interacted ones. With this assumption in mind, the authors develop a framework, named Bayesian Personalized Ranking (BPR), to perform personalized recommendations. In their framework, the observed data are transformed into a three-way binary tensor  $D$  with the first dimension representing users. The other two dimensions represent items, encoding personalized preferences between item pairs. Mathematically, this means that any first order slice of  $D$  at the  $u$ -th user,  $D_{u::}$ , is represented as a pairwise comparison matrix between items. The  $(i, j)$ -th entry when observed,  $d_{uij} \in \{-1, 1\}$ , is binary, suggesting whether  $u$ -th user prefers (or not) the  $i$ -th item over the  $j$ -th one. The tensor  $D$  is only partially observed, with missing entries where there is no prior knowledge to infer any preference for a particular user. We use 0 to indicate a missing entry. The recommendation problem becomes finding a parsimonious parameterization of the generative model for observed entries in  $D$  and estimating model parameters which best explain the observed data.

The model used in BPR assumes that among the observed entries in  $D$ , the probability that the  $u$ -th user prefers the  $i$ -th item over the  $j$ -th item can be modeled as a Bernoulli distribution,

$$p(d_{uij} = 1|\Theta) = \frac{1}{1 + \exp(-(x_{ui} - x_{uj}))}, \quad (1)$$

where  $\Theta$  is the collection of unknown parameters and  $x_{ui}$  represents the *strength* of preference on the  $i$ -th item for the  $u$ -th user. In other words, in this model, users' strengths of preference on different items are represented by scalar values denoted as  $x_{ui}$ . The relative preferences between

items are therefore characterized by the differences between their preference’s strengths for a particular user. Let

$$x_{uij} := x_{ui} - x_{uj}, \quad (2)$$

then  $x_{uij}$  becomes the natural parameter of the Bernoulli distribution and it represents  $u$ -th user’s *relative* preference on the  $i$ -th item over the  $j$ -th item.

Rendle et al. (2009) further let  $x_{ui}$  be represented as a dot product between a user vector  $\xi_u$  and an item vector  $\eta_i$ ,

$$x_{ui} = \langle \xi_u, \eta_i \rangle, \quad (3)$$

revealing the connection between their proposed BPR model and traditional matrix factorization.

Equation (1) has a direct link to the Bradley-Terry model often studied when analyzing a pairwise comparison matrix (PCM) for decision making (Hunter, 2004; Weng & Lin, 2011). This model can be at least dated back to 1929 (Zermelo, 1929). One property of the model is its transitivity: The relative preference over the  $(i, j)$ -th item pair can be expressed as the sum of relative preferences over the  $(i, t)$ -th and the  $(t, j)$ -th item pairs, for any  $t \neq i$  and  $k \neq j$ , and for any user,

$$x_{uij} = x_{uit} + x_{utj}.$$

However, in reality this transitivity property is less frequently met. Only around 3% of real world PCM’s satisfy complete transitivity (Mazurek & Perzina, 2017). The violation of the property is more conceivable when users are exposed to various types of items. For example, in an online streaming platform, one favorable movie could become less intriguing after a subscriber watches a different style/genre.

In this paper, we extend the original BPR model to allow the existence of transitivity inferred from data. In particular, we extend Equation (2) to a more general form by proposing a new tensor decomposition. We denote our new model SAD (Sliced Anti-symmetric Decomposition). The new tensor decomposition introduces a second set of non-negative item vectors  $\tau_i$  for every item. Different from the first vector  $\eta_i$ , in which entries contribute to the strength of preferences by interacting with user vector  $\xi_u$  via a dot product as in Equation (3),  $\tau_i$  extends the dot product to an *inner product*. The new vector contributes negatively when calculating relative preferences, producing counter-effects to the original strength of users’ preferences; see Section 4 for more details. The original BPR model becomes a special case of SAD when the values in  $\tau_i$  are all set to 1, and the inner product reduces to a standard dot product. When  $\tau_i$  contains entries that are not 1, the transitivity property no longer necessarily holds. While assigning an  $l_1$  regularization to the entries in  $\tau_i$  to encourage its values being 1 to reflect prior beliefs, SAD is able to infer its unknown value from real world data.

We then derive a simple and efficient group coordinate descent algorithm for parameter estimation of SAD. Our algorithm results in a simple stochastic gradient descent (SGD) producing fast and accurate parameter estimations. Through a simulation study we first demonstrate the expressiveness of SAD and efficiency of the SGD algorithm. We then compare SAD to seven alternative SOTA recommendation models in three publicly available datasets with distinct characteristics. SAD produces personalized pairwise preference more consistent with the true data.

## 2. Related Works

**Inferring priority via pairwise comparison.** The Bradley-Terry model (Zermelo, 1929; Hunter, 2004; Weng & Lin, 2011) has been heavily used along this line of research. In the Bradley-Terry model, the probability of the  $i$ -th unit (an individual, a team, or an item) being more preferable than the  $j$ -th unit (denoted as  $i \succ j$ ) is modeled by

$$p(i \succ j) = \frac{\lambda_i}{\lambda_i + \lambda_j}, \quad (4)$$

where  $\lambda_i$  represents the strength, or degree, of preference of the  $i$ -th unit. The goal is to estimate  $\lambda_i$  for all units based on pairwise comparisons. The link to Equation (1) becomes clear once we assume preference strengths of items are agnostic to users (omitting user index) and set  $x_i = \log(\lambda_i)$ . In fact, the original BPR model can be viewed as an extension to the Bradley-Terry model to allow user-specific parameters, and the strength of preferences are assumed to be dot products of user and item vectors as in Equation (3) (Rendle et al., 2009).

Various algorithms have been developed for parameter estimation of this model. For example, Hunter (2004) developed a class of algorithms named minorization-maximization (MM) for parameter estimation. In MM, a minorizing function  $Q$  is maximized to find the next parameter update at every iteration. Refer to (Hunter & Lange, 2004) for more details related to MM. Weng & Lin (2011) proposed a Bayesian approximation method to estimate team’s priorities from outputs of games between teams. Most recently, Wang et al. (2021) developed a bipartite graph iterative method to infer priorities from large and sparse pairwise comparison matrices. They applied the algorithm to the Movie-Lens dataset to rank movies based on their ratings aggregated from multiple users. Our paper is different from aforementioned models in that we model user-specific item preferences under personalized settings.

**Tensor decompositions for recommendation.** Compared to traditional collaborative filtering methods using matrix factorizations, tensor decompositions have received less attention in this field. The BPR model can be viewed as one of the first attempts to approach the recommendation problems

using tensor analysis. As discussed in Section 1, by making the assumption that interacted items are more preferable compared to non-interacted ones, user-item implicit feedback are represented as a three-way binary tensor (Rendle et al., 2009). In their later work, the authors developed tensor decomposition models for personalized tag recommendation (Rendle & Schmidt-Thieme, 2010). The relationship between their approach and traditional tensor decomposition approaches such as Tucker and PARAFAC (parallel factors) decompositions (Tucker, 1966; Kiers, 2000) was discussed.

Recently, tensor decomposition methods have been used to build recommendation systems using information from multiple sources. Wermser et al. (2011) developed a context aware tensor decomposition approach by using information from multiple sources, including time, location, and sequential information. Hidasi & Tikk (2012) considered implicit feedback and incorporated contextual information using tensor decomposition. They developed an algorithm which scaled linearly with the number of non-zero entries in a tensor. A comprehensive review about applications of tensor methods in recommendation can be found in Frolov & Oseledets (2017) and references therein. Different from leveraging multiple sources of information, the SAD model developed in this paper considers the basic scenario where only implicit feedback are available, the scenario that is considered in BPR model (Rendle et al., 2009). Our novelty lies in the fact that we propose a more general form of tensor decomposition for modeling implicit feedback.

**Deep learning in recommendation models.** Deep learning has attracted significant attention in recent years, and the recommendation domain is no exception. Traditional approaches such as collaborative filtering and factorization machines (FM) have been extended to incorporate neural network components (He et al., 2017; Chen et al., 2017; Xiao et al., 2017). In particular, Chen et al. (2017) replaced the dot product that has been widely used in traditional collaborative filtering with a neural network containing Multilayer Perceptrons (MLP) and embedding layers. Chen et al. (2017) and Xiao et al. (2017) introduced attention mechanisms (Vaswani et al., 2017) to both collaborative filtering and FM (Rendle, 2010). Mostly recently Rendle et al. (2020) revisited the comparison of traditional matrix factorization and neural collaborative filtering and concluded that matrix factorization models can be as powerful as their neural counterparts with proper hyperparameters selected. Despite the controversy, various types of deep learning models including convolutional networks, recurrent networks, variational auto-encoders (VAEs), attention models, and combinations thereof have been successfully applied in recommendation systems. Zhang et al. (2019) provided an excellent review on this topic. This line of research doesn't have direct link to the SAD model considered in the current work. However, we provide a brief review along this line since our model

could be further extended to use the latest advances in the area.

### 3. Notation

We use  $n$  to denote the total number of users in a dataset and  $m$  to denote the total number of items. Users are indexed by  $u \in [1, \dots, n]$ . Items are indexed by both  $i$  and  $j \in [1, \dots, m]$ . We use  $k$  to denote the number of latent factors, and use  $h \in [1, \dots, k]$  to index a factor. Capital letters are used to denote a matrix or a tensor, and lowercase letters to denote a scalar or a vector. For example, the three-way tensor of observations is denoted as  $D \in \mathbb{R}^{n \times m \times m}$  and the  $(u, i, j)$ -th entry is denoted as  $d_{uij}$ . Similarly, the user latent matrix is denoted as  $\Xi \in \mathbb{R}^{k \times n}$ , and its  $u$ -th column is denoted as  $\xi_u$  to represent the user vector for  $u$ -th user. We use  $\xi^h$  to denote the  $h$ -th row (the  $h$ -th factor) of  $\Xi$  viewed as a column vector.

### 4. Tensor Sliced Anti-symmetric Decomposition (SAD)

We start with the original BPR model. The relative preference  $x_{uij}$  defined in Equation (2) forms a three-way tensor  $X \in \mathbb{R}^{n \times m \times m}$  with the property:

*Property 4.1.* For every user  $u$ , the first order slice of  $X$ ,  $X_{u::}$ , is an anti-symmetric matrix, i.e.,  $X_{u::} = -X_{u::}^\top$ .

This can be shown easily by letting  $p_{uij} = p(d_{uij} = 1) = p(i \succ_u j)$  and noting that the relative preference  $x_{uij}$  is the natural parameter of the corresponding Bernoulli distribution with

$$x_{uij} = \log \left( \frac{p_{uij}}{1 - p_{uij}} \right).$$

Note that  $x_{uij}$  is also known as the log-odds or logit.

#### 4.1. Parsimonious representation of $X_{u::}$

The decomposition introduced in the BPR model (Rendle et al., 2009) can be viewed as one parsimonious representation of the first order slices of  $X$ . Let  $\xi_u \in \mathbb{R}^k$  and  $\eta_i \in \mathbb{R}^k$  denote the user and item vectors respectively, and let  $\xi_{hu}$  ( $\eta_{hi}$ ) indicate the  $h$ -th entry in  $\xi_u$  ( $\eta_i$ ). Equations (1), (2), and (3) can be re-written as

$$\begin{aligned} X_{u::} &= \sum_{h=1}^k \xi_{hu} \begin{pmatrix} 0 & \eta_{h1} - \eta_{h2} & \cdots & \eta_{h1} - \eta_{hm} \\ \eta_{h2} - \eta_{h1} & 0 & \cdots & \eta_{h2} - \eta_{hm} \\ \vdots & \vdots & \ddots & \vdots \\ \eta_{hm} - \eta_{h1} & \eta_{hm} - \eta_{h2} & \cdots & 0 \end{pmatrix} \\ &= \sum_{h=1}^k \xi_{hu} (\tilde{H}_h - (\tilde{H}_h)^\top), \end{aligned}$$

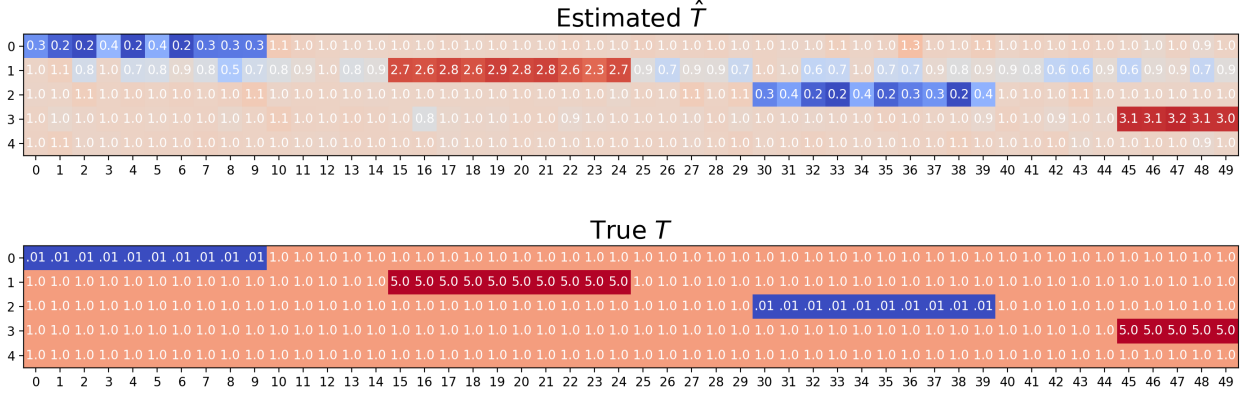


Figure 1. Comparison of  $\hat{T}$  with ground truth. Factors are re-ordered in  $\hat{T}$  to match true  $T$ .

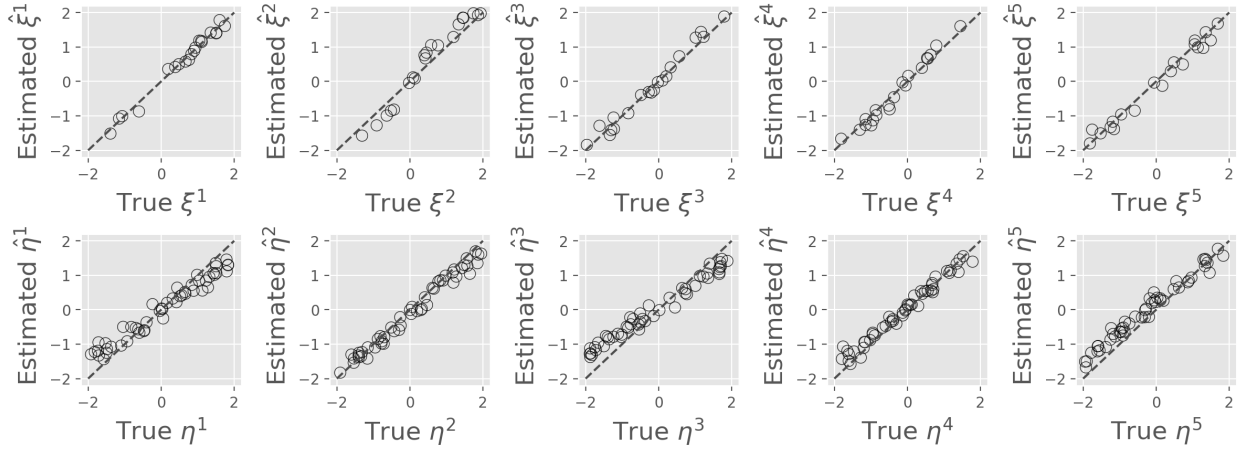


Figure 2. Comparison of  $\hat{\Xi}, \hat{H}$  with their ground truth. Factors are re-ordered and signs are flipped to match true parameter.

where

$$\tilde{H}_h = \begin{pmatrix} \eta_{h1} & \eta_{h1} & \cdots & \eta_{h1} \\ \eta_{h2} & \eta_{h2} & \cdots & \eta_{h2} \\ \vdots & \vdots & \ddots & \vdots \\ \eta_{hm} & \eta_{hm} & \cdots & \eta_{hm} \end{pmatrix} = \eta^h \circ \mathbb{1},$$

with  $\mathbb{1} \in \mathbb{R}^m$  being a vector of all 1's,  $\eta^h \in \mathbb{R}^m$  being the  $h$ -th row of item matrix  $H \in \mathbb{R}^{k \times m}$ , and  $\circ$  being the outer product.

With the above definition, we have

$$X_{u::} = \sum_{h=1}^k \xi_{hu} (\eta^h \circ \mathbb{1} - \mathbb{1} \circ \eta^h). \quad (5)$$

The above decomposition suggests that for the  $u$ -th user, her item preference matrix  $X_{u::}$  can be decomposed as a weighted sum of  $k$  anti-symmetric components, each of

which is the difference of a rank one square matrix and its transpose.

## 4.2. Generalization of BPR

By replacing  $\mathbb{1}$  with arbitrary vector  $\tau^h \in \mathbb{R}^m$ , the new square matrix  $\eta^h \circ \tau^h - \tau^h \circ \eta^h$  is still anti-symmetric, and Property 4.1 still holds for the resulting  $X_{u::}$ . In this work we require entries in  $\tau^h$  to be non-negative. The rationale will become clear in Section 4.3.

With this observation, we generalize Equation (5) by proposing a new parsimonious representation of  $X_{u::}$ ,

$$X_{u::} = \sum_{h=1}^k \xi_{hu} (\eta^h \circ \tau^h - \tau^h \circ \eta^h). \quad (6)$$

Furthermore, by letting  $\Xi := (\xi_1, \xi_2, \dots, \xi_n) \in \mathbb{R}^{k \times n}$ ,  $H := (\eta^1, \eta^2, \dots, \eta^k)^\top \in \mathbb{R}^{k \times m}$ , and  $T :=$



$(\tau^1, \tau^2, \dots, \tau^k)^\top \in \mathbb{R}_+^{k \times m}$  (we use  $\mathbb{R}_+$  to denote the set of non-negative real numbers), we introduce the proposed Sliced Anti-symmetric Decomposition (SAD).

**Definition 4.1.** We define the Sliced Anti-symmetric Decomposition (SAD) of  $X$  to be the matrices  $\Xi, H, T$  satisfying Equation (6) above for every user index  $u$ . We denote this by

$$X \stackrel{\text{SAD}}{:=} [\Xi, H, T]. \quad (7)$$

### 4.3. Interpretation of SAD

To understand the interpretation of SAD, we re-write the original equations (2) and (3) as

$$x_{uij} = \langle \xi_u, \eta_i \rangle - \langle \xi_u, \eta_j \rangle = \sum_{h=1}^k (\xi_{hu} \eta_{hi} - \xi_{hu} \eta_{hj}).$$

The term  $\xi_{hu} \eta_{hi}$  can be interpreted as the strength of preference of the  $u$ -th user on the  $i$ -th item from the  $h$ -th factor. The overall strength of preference,  $x_{ui}$ , is the sum of contributions from the  $k$  individual factors. Accordingly, the relative preference over the  $(i, j)$ -th item pair for the  $u$ -th user can be viewed as the difference between the preference strengths of the  $i$ -th and the  $j$ -th items from the  $u$ -th user.

This interpretation has a direct link to the Bradley-Terry model (Equation (4)) as previously mentioned, in which the strength of the  $i$ -th item is described as a positive number  $\lambda_i$ . Here the strength of preference is viewed as user specific and is represented by a real number  $x_{ui} = \log \lambda_{ui}$ .

SAD extends the original equations (2) and (3) by introducing a new non-negative vector  $\tau_i$  for every item. We can re-write Equation (6) as

$$x_{uij} = \langle \xi_u, \eta_i \rangle_{\text{diag}(\tau_j)} - \langle \xi_u, \eta_j \rangle_{\text{diag}(\tau_i)} \quad (8)$$

$$= \sum_{h=1}^k (\xi_{hu} \eta_{hi} \tau_{hj} - \xi_{hu} \eta_{hj} \tau_{hi}). \quad (9)$$

$\langle \cdot, \cdot \rangle_{\text{diag}(\tau_i)}$  in Equation (8) denotes the inner product with a diagonal weight matrix having  $\tau_i$  on the diagonal. To be a proper inner product, we require the entries in  $\tau_i$  to be non-negative, resulting in a positive semi-definite weight matrix  $\text{diag}(\tau_i)$ .

The first term on the right hand side of Equation (9), describing the preference strength of the  $i$ -th item, now becomes dependent on  $\tau_{hj}$ , the  $h$ -th entry in  $\tau_j$  of the  $j$ -th rival. When  $\tau_{hj}$  is bigger than 1, it increases the effect of  $\xi_{hu} \eta_{hi}$ . Similarly, the second term on the right hand side suggests that when  $\tau_{hi}$  is bigger than 1, it strengthens the effect of the  $j$ -th item. The opposites happen when either  $\tau_{hj}$  or  $\tau_{hi}$  is smaller than 1. Therefore, the new non-negative item vector

$\tau_i$  can be viewed as a counter-effect acting upon the strength of relative preferences, penalizing the strength when it is greater than 1, while reinforcing when it is smaller than 1.

SAD's generalization allows items to interact with each other when a user exhibits her preference. In real world applications, a user's preference indeed may be influenced by different items. For example, during online shopping, one favorable dress may become less intriguing after a customer sees a different one with different style/color that matches her needs. In an online streaming platform, one favorable movie could become less interesting after a subscriber watches another one with different style/genre. SAD allows us to capture these item-item interactions by introducing a new set of vectors  $\tau_i$ .

To summarize, we interpret the three factor matrices in SAD as follows:

- $\Xi$  represents the user matrix. Each user is represented by a  $k$ -dimensional user vector  $\xi_u \in \mathbb{R}^k$ .
- $H$  represents the *left* item matrix, which is composed of *left* item vectors denoted as  $\eta_i \in \mathbb{R}^k$ . It contributes to the strength of preference on the  $i$ -th item via an inner product with user vector  $\xi_u$ .
- $T$  represents the *right* item matrix, which contains non-negative *right* item vectors denoted as  $\tau_i \in \mathbb{R}_+^k$ . This set of vectors defines the weight matrices of inner products between  $\eta_i$  and  $\xi_u$ . It produces counter-effects to the original preference strengths, with values bigger than 1 adding additional strength to rival items in pairwise comparisons, and a value smaller than 1 producing the opposite effect. When  $T = 1$ , the model reduces to the original BPR model.

In SAD we estimate the value of  $T$  from data by adding an  $l_1$  regularization centered around 1 to the entries in  $T$  independently. Doing this we effectively let SAD learn the values of  $T$  from data.

### 4.4. The transitivity problem

In social science involving decision makings, pairwise comparison matrices (PCMs) have been investigated extensively (Saaty & Vargas, 2013; Wang et al., 2021). It is usually assumed that a PCM meets the transitivity property, resulting in the following property introduced in Section 1: The relative preference of the  $(i, j)$ -th item pair can be derived from the sum of relative preferences of the  $(i, t)$ -th and  $(t, j)$ -th item pairs, with  $t \neq i$  and  $t \neq j$ ,  $x_{uij} = x_{uit} + x_{utj}$ . The original BPR meets this property nicely. After introducing  $T$  in SAD, this property is no longer necessarily met. One can show that  $\tau_i = \tau_j = \tau_t$  for ternary  $(i, j, t)$  is a sufficient condition for transitivity in SAD. Since complete transitivity

is met only in 3% of real world applications (Mazurek & Perzina, 2017), SAD allows this property to be estimated from data, making the proposed model more realistic.

#### 4.5. Inference algorithms

To estimate model parameters, we maximize the log likelihood function directly. The log likelihood given observed entries in  $D$  can be re-written as

$$\begin{aligned} \log p(D|\Theta) &= \sum_{(u,i,j)} \log p(d_{uij}|x_{uij}) \\ &= \sum_{(u,i,j)} \left[ \mathbf{1}(d_{uij} = 1) \log \left( \frac{1}{1 + \exp(-x_{uij})} \right) \right. \\ &\quad \left. + \mathbf{1}(d_{uij} = -1) \log \left( \frac{\exp(-x_{uij})}{1 + \exp(-x_{uij})} \right) \right] \\ &= \sum_{(u,i,j)} \mathbf{1}(d_{uij} = -1) x_{uij} - \log(1 + \exp(-x_{uij})), \end{aligned}$$

where  $\mathbf{1}(\cdot)$  is the indicator function, and the sum is taken with respect to non-missing entries in  $D$  and  $i < j$ . Here we require  $i < j$  to prevent us from double counting.

We take the derivatives with respect to the columns of  $\Xi$ ,  $H$ , and  $T$ , resulting in following gradients

$$\begin{aligned} \frac{\partial \log p(D|\Theta)}{\partial \xi_u} &= w_{uij}(\eta_i \odot \tau_j - \eta_j \odot \tau_i), \\ \frac{\partial \log p(D|\Theta)}{\partial \eta_i} &= w_{uij} \xi_u \odot \tau_j, \\ \frac{\partial \log p(D|\Theta)}{\partial \eta_j} &= -w_{uij} \xi_u \odot \tau_i, \\ \frac{\partial \log p(D|\Theta)}{\partial \tau_i} &= -w_{uij} \xi_u \odot \eta_j, \\ \frac{\partial \log p(D|\Theta)}{\partial \tau_j} &= w_{uij} \xi_u \odot \eta_i, \end{aligned} \quad (10)$$

from the  $(u, i, j)$ -th observation. Here

$$w_{uij} = \mathbf{1}(d_{uij} = -1) + \exp(-x_{uij}) / (1 + \exp(-x_{uij}))$$

and  $\odot$  is the element-wise product (Hadamard product).

Equation (10) allows us to create a stochastic gradient descent (SGD) algorithm to optimize the negative of the log likelihood. During optimization, we add an  $l_1$  penalty with weight  $w_1$  to the entries in  $T$  independently to encourage their values to be 1. In addition, we add an  $l_2$  independent penalties with weight  $w_2$  to both  $\Xi$  and  $H$  for further regularization.

We also develop an efficient Gibbs sampling algorithm for full posterior inference under a Probit model setup. By drawing parameter samples from posterior distributions, the Gibbs sampling algorithm has the advantage of producing

accurate uncertainty estimation of the unknown parameters under Bayesian inference. We replace the logistic function in Equation (1) with

$$p(d_{uij} = 1|\Theta) = \Phi(x_{uij}),$$

where  $\Phi(x_{uij})$  is the cumulative distribution function (CDF) of the standard Gaussian distribution centered at  $x_{uij}$ . By assigning spherical Gaussian priors to  $\Xi$ ,  $H$ , and  $T$ , full conditional distributions can be derived. More details can be found in Appendix A.

## 5. Simulation Study

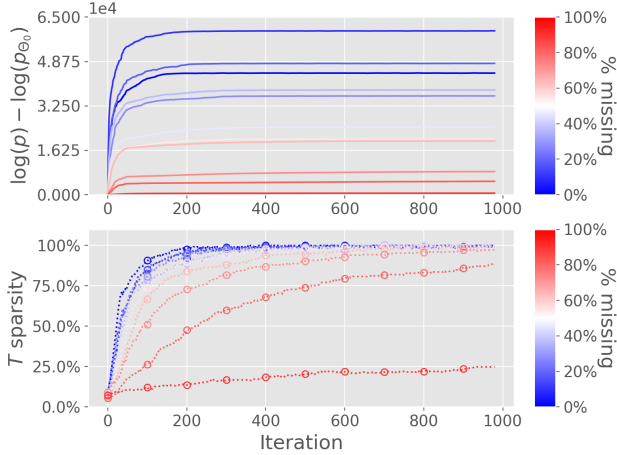
We first evaluate the performance of SAD and the SGD algorithm on simulation data. We choose  $n = 20$  users,  $m = 50$  items, and  $k = 5$  and consider two scenarios. In the first simulation (Sim1) we set  $T$  to 1, effectively reducing SAD to the generative model of BPR (Rendle et al., 2009). In the second scenario (Sim2), we set a small proportion of  $T$  to either 0.01 or 5, the other entries are set to 1. For user matrix  $\Xi$  and left item matrix  $H$ , their values are uniformly drawn from the interval  $[-2, 2]$ . We calculate the preference tensor  $X$  with Equation (8) and draw an observation tensor  $D$  from the corresponding Bernoulli distributions.

We first examine the performance of SAD with complete observations in Sim2 to validate if our method is able to generate accurate parameter estimation. We run the SGD algorithm with a learning rate 0.05. The weight of the  $l_1$  regularization assigned to  $T$  is set to 0.01, and the weight of the  $l_2$  regularization is set to 0.005. Initial values of parameters are randomly drawn from a standard Gaussian distribution. The number of latent factors  $k$  is set to the true value. After 20 epochs,  $\hat{T}$  is able to recover the sparse structure of the true parameters of  $T$  up to permutation of factors (Figure 1). The user matrix and left item matrix converge to the true parameter values as well (Figure 2).

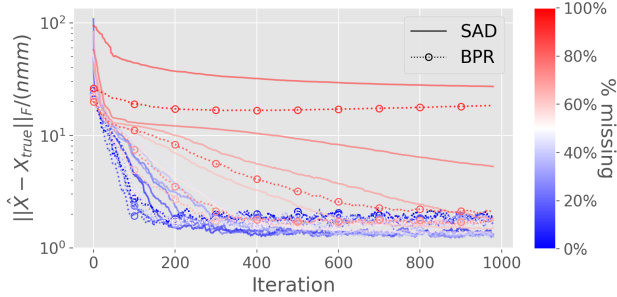
Next we examine the performance of SAD in both Sim1 and Sim2, under the scenarios with missing data. To be more specific, we randomly mark  $x\%$  of  $D$  as missing to mimic missing at random. Note that in the real world, observations could have more complex missingness structures. As a comparison, we run BPR under the same contexts.

The convergences of SAD in Sim1 are shown in Figure 3(a), together with the estimated sparsity of  $T$ . Here the sparsity of  $T$  is defined as the percentage of the entries in  $T$  with  $|\tau_{hj} - 1| < 0.05$ . When the percentage of missingness is at small or medium levels, SAD is able to converge to a sparsity close to 1, suggesting the effectiveness of the  $l_1$  regularization. It becomes more challenging when the percentage of missingness surpasses 70%. Figure 3(b) shows the trajectories of the mean squared error (MSE) between  $\hat{X}$  and the true  $X$  under different missingness percentages

for both SAD and BPR. Both SAD and BPR are able to converge to a low MSE with small/medium percentages of missingness. Similarly, with a high percentage of missingness, the performance of both models begins to deteriorate. We conclude that SAD has a performance *on par* with BPR when data are simulated from the generative model of BPR.



(a) Convergence of SAD and its sparsity. Y-axis in first row shows the changes of log likelihood to its initial value with randomly initialized parameters  $\Theta_0$  during model fitting.



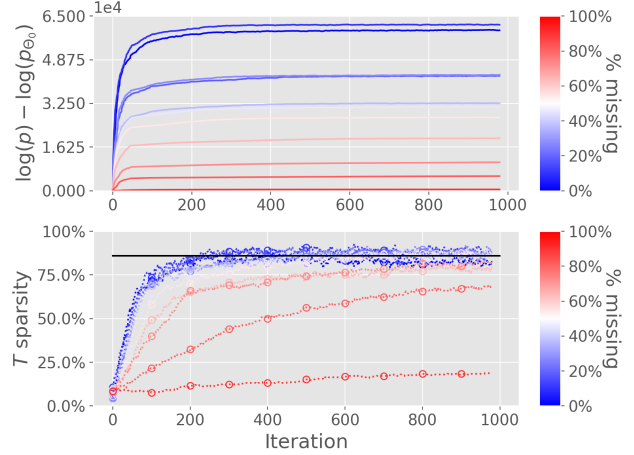
(b) Convergence of SAD and BPR

Figure 3. Evaluation of SAD and BPR with missing data in Sim1.

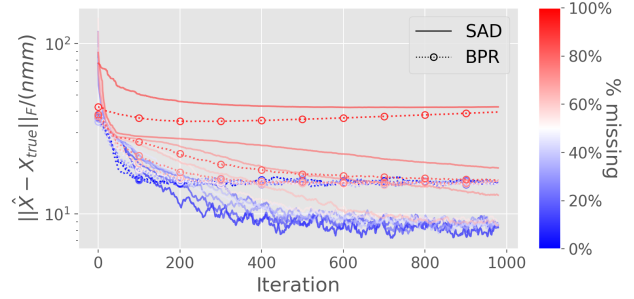
Results for Sim2 are shown in Figure 4. Note that the true sparsity of  $T$  is 86%. SAD is able to generate an accurate estimation of the sparsity under small/medium percentages of missingness (Figure 4(a)). When evaluating both models using MSE, SAD is able to achieve a much lower value due to its correct specification of the generative model (Figure 4(b)).

## 6. Applications for Real Data

We select three real world datasets to evaluate SAD and compare against SOTA recommendation models. The first dataset used is from the Netflix Prize (Bennett et al., 2007). The original dataset contains movie ratings of 8,921 movies from 478,533 unique users, with a total number of ratings



(a) Convergence of SAD and its sparsity. Y-axis in first row shows the changes of log likelihood to its initial value with randomly initialized parameters  $\Theta_0$  during model fitting.



(b) Convergence of SAD and BPR

Figure 4. Evaluation of SAD and BPR with missing data in Sim2. The horizontal line shown in second row of 4(a) marks the true sparsity of  $T$ .

reaching to over 50M. We randomly select 10,000 users as our first dataset. The resulting dataset contains 8,693 movies with over 1M ratings from the 10,000 users. For the second dataset, we choose the Movie-Lens 1M dataset (Harper & Konstan, 2015). It contains over 1M ratings from 6,040 users on 3,706 movies. As a third dataset, we consider the reviews of Fine-Foods from Amazon (McAuley & Leskovec, 2013). The complete dataset has 0.5M reviews from 256K users on 74K food products. We select the top 10,000 users with the most reviews, resulting in 162K reviews on 30K items.

The three datasets have distinct characteristics. Among the three datasets, the Amazon food review dataset has the least user-item interactions, even when the most active users are selected. The maximum number of items viewed by a single user is 448. It also has the largest number of items. The Netflix dataset is the most skewed, with the number of items interacted by a user ranging from as low as 1 to as high as over 8K. The Movie-Lens dataset contains the largest

Dataset	Model	Mean	Std	P-value	$\log(p)^*$
Netflix	SAD	0.16	1.45	0.0	-466.90
	BPR	-0.02	2.73	0.0	-479.81
	SVD	-0.01	2.16	0.0	-1919.86
	MF	-0.01	4.41	0.0	-9288.57
	PMF	-0.01	1.03	0.0	-2019.39
	FM	0.04	2.06	0.0	-375.69
	NCF	-0.12	2.82	0.0	-39.98
	$\beta$ -VAE	-0.02	2.79	0.0	-3915.77
Movie -Lens	SAD	0.41	1.41	0.0	-3007.04
	BPR	0.19	0.77	0.0	-2677.18
	SVD	0.33	1.78	0.0	-1370.25
	MF	0.01	2.44	0.0	-15816.47
	PMF	0.09	0.84	0.0	-9466.90
	FM	0.19	3.64	0.0	-2050.33
	NCF	0.16	3.02	0.0	-1387.03
	$\beta$ -VAE	0.01	2.19	0.0	-15728.44
Amazon Food	SAD	0.03	1.53	9.8e-65	-297.42
	BPR	-0.06	0.59	0.0	-110.82
	SVD	-0.69	7.06	0.0	-207.94
	MF	2.3e-3	2.00	0.24	-1402.18
	PMF	-5.6e-3	0.75	1.6e-13	-469.32
	FM	-0.03	1.67	1.4e-60	-29.11
	NCF	1.0e-3	0.25	9.6e-5	-411.73
	$\beta$ -VAE	-9.2e-3	2.25	6.6e-5	-369.92

Table 1. Comparisons of different models on real world datasets. A higher value of mean suggests a model produces predictions more consistent with ground truth (see text for details).  $\log(p)$  is calculated from a fixed set of randomly selected 100 users.

number of user-item interactions, and is most uniformly distributed. Some details of the three datasets can be found in Table 2 in Appendix B.

We choose seven SOTA recommendation models to compare with SAD. Their details are listed in Table 3 in Appendix C. We perform a grid search on a range of hyper-parameters and report the resulting model that fits best to the three datasets based on the Bernoulli likelihood in Equation (1). We set  $k = 5,000$  in the Netflix dataset,  $k = 3,000$  in the Movie-Lens dataset, and  $k = 4,000$  in Amazon Food review dataset. During evaluation, we use the explicit ratings from the three datasets and examine whether the models are able to produce relative preferences that are consistent with the data. Specifically, we extract item pairs with known preferences ( $i \succ j$ ) for all users, resulting in 103, 876, 216 pairs from the Netflix dataset, 137, 122, 777 pairs from the Movie-Lens dataset, and 951, 529 pairs from Amazon Food review dataset. We evaluate models by calculating the mean, standard deviation (std), and statistical significance of the estimated relative preferences for those item pairs. Models that produce positive relative preferences fit more consistently to the data. This means that we expect higher means for more consistent models. SAD produces the most consistent relative preferences for all three datasets (Table 1). Table 4 in Appendix D illustrates examples in which SAD pro-

duces model predictions consistent with true ratings while the SOTA model fails.

## 7. Discussions

In this paper we propose a new tensor decomposition approach for collaborative filtering with implicit feedback. In contrast to traditional models, we introduce a new set of non-negative latent vectors for items. The new vectors generalize the standard dot products for calculating user-item preferences to general inner products, allowing interactions to exist between items when evaluating their relative preferences. When such vectors are all set to 1’s, our model reduces to standard collaborative filtering models. We allow the values of such vectors to be learned from data, resulting in personalized pairwise preferences more consistent with real world data.

Producing personalized rankings is another important topic when building recommendation systems. With one latent representation for users and items, a deterministic strength of preference can be calculated for every item and every user. The value of the strength naturally becomes a score to produce personalized rankings. The new vectors introduced in our model add obscurities, since the strength of preference becomes dependent on another rival item. One possible approach is to aggregate left and right item vectors into a single one and use the aggregation to determine the preference strength. Another approach could be viewing the right item vectors as evaluation contexts. A stability measure from the contexts can be derived for each item, and such a measure can be used to penalize the preference strengths calculated using left item vectors. This topic is currently under investigation.

The framework developed in this paper can be easily extended to use the latest advances in deep learning. We expect the expressiveness of SAD could be further enhanced when neural network components are integrated into the framework.

## References

- Bennett, J., Lanning, S., et al. The Netflix prize. In *Proceedings of KDD Cup and Workshop*, volume 2007, pp. 35. New York, NY, USA., 2007.
- Chen, J., Zhang, H., He, X., Nie, L., Liu, W., and Chua, T.-S. Attentive collaborative filtering: Multimedia recommendation with item-and component-level attention. In *Proceedings of the 40th International ACM SIGIR Conference on Research and Development in Information Retrieval*, pp. 335–344, 2017.
- Frolov, E. and Oseledets, I. Tensor methods and recom-



- mender systems. *Wiley Interdisciplinary Reviews: Data Mining and Knowledge Discovery*, 7(3):e1201, 2017.
- Graham, S., Min, J.-K., and Wu, T. Microsoft recommenders: Tools to accelerate developing recommender systems. In *Proceedings of the 13th ACM Conference on Recommender Systems*, pp. 542–543, 2019.
- Harper, F. M. and Konstan, J. A. The Movielens datasets: History and context. *ACM Transactions on Interactive Intelligent Systems (TIIS)*, 5(4):1–19, 2015.
- He, X., Liao, L., Zhang, H., Nie, L., Hu, X., and Chua, T.-S. Neural collaborative filtering. In *Proceedings of the 26th International Conference on World Wide Web*, pp. 173–182, 2017.
- Hidasi, B. and Tikk, D. Fast ALS-based tensor factorization for context-aware recommendation from implicit feedback. In *Joint European Conference on Machine Learning and Knowledge Discovery in Databases*, pp. 67–82. Springer, 2012.
- Hu, Y., Koren, Y., and Volinsky, C. Collaborative filtering for implicit feedback datasets. In *2008 Eighth IEEE International Conference on Data Mining*, pp. 263–272. Ieee, 2008.
- Hug, N. Surprise: A Python library for recommender systems. *Journal of Open Source Software*, 5(52):2174, 2020. doi: 10.21105/joss.02174. URL <https://doi.org/10.21105/joss.02174>.
- Hunter, D. R. MM algorithms for generalized Bradley-Terry models. *The Annals of Statistics*, 32(1):384–406, 2004.
- Hunter, D. R. and Lange, K. A tutorial on MM algorithms. *The American Statistician*, 58(1):30–37, 2004.
- Kiers, H. A. Towards a standardized notation and terminology in multiway analysis. *Journal of Chemometrics: A Journal of the Chemometrics Society*, 14(3):105–122, 2000.
- Liang, D., Krishnan, R. G., Hoffman, M. D., and Jebara, T. Variational autoencoders for collaborative filtering. In *Proceedings of the 2018 World Wide Web Conference*, pp. 689–698, 2018.
- Mazurek, J. and Perzina, R. On the inconsistency of pairwise comparisons: An experimental study. *Scientific Papers of the University of Pardubice. Series D, Faculty of Economics and Administration*, 2017.
- McAuley, J. J. and Leskovec, J. From amateurs to connoisseurs: Modeling the evolution of user expertise through online reviews. In *Proceedings of the 22nd International Conference on World Wide Web*, pp. 897–908, 2013.
- Mnih, A. and Salakhutdinov, R. R. Probabilistic matrix factorization. In *Advances in Neural Information Processing Systems*, pp. 1257–1264, 2008.
- Pan, R., Zhou, Y., Cao, B., Liu, N. N., Lukose, R., Scholz, M., and Yang, Q. One-class collaborative filtering. In *2008 Eighth IEEE International Conference on Data Mining*, pp. 502–511. IEEE, 2008.
- Rendle, S. Factorization machines. In *2010 IEEE International Conference on Data Mining*, pp. 995–1000, 2010. doi: 10.1109/ICDM.2010.127.
- Rendle, S. and Schmidt-Thieme, L. Pairwise interaction tensor factorization for personalized tag recommendation. In *Proceedings of the Third ACM International Conference on Web Search and Data Mining*, pp. 81–90, 2010.
- Rendle, S., Freudenthaler, C., Gantner, Z., and Schmidt-Thieme, L. BPR: Bayesian personalized ranking from implicit feedback. In *Proceedings of the Twenty-Fifth Conference on Uncertainty in Artificial Intelligence*, pp. 452–461, 2009.
- Rendle, S., Krichene, W., Zhang, L., and Anderson, J. Neural collaborative filtering vs. matrix factorization revisited. In *Fourteenth ACM Conference on Recommender Systems*, pp. 240–248, 2020.
- Saaty, T. L. and Vargas, L. G. The analytic network process. In *Decision Making with the Analytic Network Process*, pp. 1–40. Springer, 2013.
- Salah, A., Truong, Q.-T., and Lauw, H. W. Cornac: A comparative framework for multimodal recommender systems. *the Journal of Machine Learning Research*, 21: 1–5, 2020.
- Tucker, L. R. Some mathematical notes on three-mode factor analysis. *Psychometrika*, 31(3):279–311, 1966.
- Vaswani, A., Shazeer, N., Parmar, N., Uszkoreit, J., Jones, L., Gomez, A. N., Kaiser, Ł., and Polosukhin, I. Attention is all you need. In *Advances in Neural Information Processing Systems*, pp. 5998–6008, 2017.
- Wang, H., Kou, G., and Peng, Y. An iterative algorithm to derive priority from large-scale sparse pairwise comparison matrix. *IEEE Transactions on Systems, Man, and Cybernetics: Systems*, 2021.
- Weng, R. C. and Lin, C.-J. A Bayesian approximation method for online ranking. *Journal of Machine Learning Research*, 12(1), 2011.
- Wermser, H., Rettinger, A., and Tresp, V. Modeling and learning context-aware recommendation scenarios using tensor decomposition. In *2011 International Conference*

on *Advances in Social Networks Analysis and Mining*, pp. 137–144. IEEE, 2011.

Xiao, J., Ye, H., He, X., Zhang, H., Wu, F., and Chua, T.-S. Attentional factorization machines: Learning the weight of feature interactions via attention networks. In *Proceedings of the 26th International Joint Conference on Artificial Intelligence, IJCAI'17*, pp. 3119–3125, Melbourne, Australia, 2017. AAAI Press. ISBN 978-0-9992411-0-3.

Zermelo, E. Die berechnung der turnier-ergebnisse als ein maximumproblem der wahrscheinlichkeitsrechnung. *Mathematische Zeitschrift*, 29(1):436–460, 1929.

Zhang, S., Yao, L., Sun, A., and Tay, Y. Deep learning based recommender system: A survey and new perspectives. *ACM Computing Surveys*, 52(1):1–38, 2019.

## A. Gibbs Sampler for Posterior Inference of SAD

We derive an efficient Gibbs sampling algorithm as a complement to the SGD algorithm in the main paper. The Gibbs sampling algorithm has the advantage of producing accurate uncertainty estimation of unknowns under Bayesian inference by drawing parameter samples from the posterior distribution. The algorithm is an application of Bayesian Probit regression to the current setting. Specifically, we replace the original logistic parameterization in Equation (1) with the following equation:

$$p(d_{uij} = 1 | \Theta) := \Phi(x_{uij}), \quad (11)$$

where  $\Phi(x_{uij})$  is the CDF of a Gaussian distribution with mean  $x_{uij}$  and variance 1. By augmenting the model with a hidden tensor  $Z = \{z_{uij}\}$ , where  $z_{uij} = x_{uij} + \epsilon_{uij}$  and  $\epsilon_{uij} \stackrel{\text{i.i.d.}}{\sim} N(0, 1)$ , the Probit model is equivalent to

$$d_{uij} = \begin{cases} 1 & z_{uij} > 0 \\ -1 & z_{uij} \leq 0 \end{cases}.$$

With this new model, an efficient Gibbs sampling algorithm can be derived. As a toy example, we assign spherical Gaussian priors to rows of  $\Xi$ ,  $H$  and  $T$  independently. With the likelihood defined in Equation (11), the following conditional posterior distributions can be derived.

### Posterior of $z_{uij}$

$$z_{uij} | \Xi, H, T \sim \begin{cases} N_+(x_{uij}, 1) & \text{if } d_{uij} = 1 \\ N_-(x_{uij}, 1) & \text{if } d_{uij} = -1 \end{cases},$$

where  $N_+(\mu, \sigma)$  and  $N_-(\mu, \sigma)$  are truncated Gaussian distributions on positive and negative quadrants respectively.

### Posterior of $\xi_u$ with $u = 1, \dots, n$

$$\xi_u | Z, \Xi \setminus \xi_u, H, T \sim N_k(\Sigma_u^\xi (\Psi_u^\xi)^\top \bar{z}_u^\xi, \Sigma_u^\xi),$$

where  $(\Sigma_u^\xi)^{-1} = (\Psi_u^\xi)^\top (\Psi_u^\xi) + I$ ,

$$\Psi_u^\xi = \begin{pmatrix} \eta_{11}\tau_{12} - \eta_{12}\tau_{11} & \eta_{21}\tau_{22} - \eta_{22}\tau_{21} & \cdots & \eta_{k1}\tau_{k2} - \eta_{k2}\tau_{k1} \\ \eta_{11}\tau_{13} - \eta_{13}\tau_{11} & \eta_{21}\tau_{23} - \eta_{23}\tau_{21} & \cdots & \eta_{k1}\tau_{k3} - \eta_{k3}\tau_{k1} \\ \vdots & \vdots & \ddots & \vdots \\ \eta_{12}\tau_{13} - \eta_{13}\tau_{12} & \eta_{22}\tau_{23} - \eta_{23}\tau_{22} & \cdots & \eta_{k2}\tau_{k3} - \eta_{k3}\tau_{k2} \\ \vdots & \vdots & \ddots & \vdots \\ \eta_{1,m-1}\tau_{1m} - \eta_{1m}\tau_{1,m-1} & \eta_{2,m-1}\tau_{2m} - \eta_{2m}\tau_{2,m-1} & \cdots & \eta_{k,m-1}\tau_{km} - \eta_{km}\tau_{k,m-1} \end{pmatrix} \in \mathbb{R}^{m(m-1)/2 \times k},$$

and  $\bar{z}_u^\xi = [z_{u12}, z_{u13}, \dots, z_{u23}, z_{u24}, \dots, z_{u,m-1,m}]^\top \in \mathbb{R}^{m(m-1)/2}$ .

### Posterior of $\eta_i$ with $i = 1, \dots, m$

$$\eta_i | Z, \Xi, H \setminus \eta_i, T \sim N_k(\Sigma_i^\eta (\Psi_i^\eta)^\top \bar{z}_i^\eta, \Sigma_i^\eta),$$

where  $(\Sigma_i^\eta)^{-1} = (\Psi_i^\eta)^\top (\Psi_i^\eta) + I$ ,

$$\Psi_i^\eta = \begin{pmatrix} \xi_{11}\tau_{11} & \xi_{21}\tau_{21} & \cdots & \xi_{k1}\tau_{k1} \\ \xi_{11}\tau_{12} & \xi_{21}\tau_{22} & \cdots & \xi_{k1}\tau_{k2} \\ \vdots & \vdots & \ddots & \vdots \\ \xi_{11}\tau_{1,i-1} & \xi_{21}\tau_{2,i-1} & \cdots & \xi_{k1}\tau_{k,i-1} \\ \xi_{11}\tau_{1,i+1} & \xi_{21}\tau_{2,i+1} & \cdots & \xi_{k1}\tau_{k,i+1} \\ \vdots & \vdots & \ddots & \vdots \\ \xi_{11}\tau_{1m} & \xi_{21}\tau_{2m} & \cdots & \xi_{k1}\tau_{km} \\ \xi_{12}\tau_{11} & \xi_{22}\tau_{21} & \cdots & \xi_{k2}\tau_{k1} \\ \vdots & \vdots & \ddots & \vdots \\ \xi_{12}\tau_{1,i-1} & \xi_{22}\tau_{2,i-1} & \cdots & \xi_{k2}\tau_{k,i-1} \\ \xi_{12}\tau_{1,i+1} & \xi_{22}\tau_{2,i+1} & \cdots & \xi_{k2}\tau_{k,i+1} \\ \vdots & \vdots & \ddots & \vdots \\ \xi_{12}\tau_{1m} & \xi_{22}\tau_{2m} & \cdots & \xi_{k2}\tau_{km} \\ \vdots & \vdots & \ddots & \vdots \\ \xi_{1n}\tau_{11} & \xi_{2n}\tau_{21} & \cdots & \xi_{kn}\tau_{k1} \\ \vdots & \vdots & \ddots & \vdots \\ \xi_{1n}\tau_{1,i-1} & \xi_{2n}\tau_{2,i-1} & \cdots & \xi_{kn}\tau_{k,i-1} \\ \xi_{1n}\tau_{1,i+1} & \xi_{2n}\tau_{2,i+1} & \cdots & \xi_{kn}\tau_{k,i+1} \\ \vdots & \vdots & \ddots & \vdots \\ \xi_{1n}\tau_{1m} & \xi_{2n}\tau_{2m} & \cdots & \xi_{kn}\tau_{km} \end{pmatrix} \in \mathbb{R}^{n(m-1) \times k},$$

and

$$\bar{z}_i^\eta = \begin{pmatrix} z_{1i1} + \sum_{h=1}^k \xi_{h1}\tau_{hi}\eta_{h1} \\ z_{1i2} + \sum_{h=1}^k \xi_{h1}\tau_{hi}\eta_{h2} \\ \vdots \\ z_{1,i,i-1} + \sum_{h=1}^k \xi_{h1}\tau_{hi}\eta_{h,i-1} \\ z_{1,i,i+1} + \sum_{h=1}^k \xi_{h1}\tau_{hi}\eta_{h,i+1} \\ \vdots \\ z_{1im} + \sum_{h=1}^k \xi_{h1}\tau_{hi}\eta_{h,m} \\ z_{2i1} + \sum_{h=1}^k \xi_{h2}\tau_{hi}\eta_{h1} \\ \vdots \\ z_{2,i,i-1} + \sum_{h=1}^k \xi_{h2}\tau_{hi}\eta_{h,i-1} \\ z_{2,i,i+1} + \sum_{h=1}^k \xi_{h2}\tau_{hi}\eta_{h,i+1} \\ \vdots \\ z_{2im} + \sum_{h=1}^k \xi_{h2}\tau_{hi}\eta_{h,m} \\ \vdots \\ z_{ni1} + \sum_{h=1}^k \xi_{hn}\tau_{hi}\eta_{h1} \\ \vdots \\ z_{n,i,i-1} + \sum_{h=1}^k \xi_{hn}\tau_{hi}\eta_{h,i-1} \\ z_{n,i,i+1} + \sum_{h=1}^k \xi_{hn}\tau_{hi}\eta_{h,i+1} \\ \vdots \\ z_{nim} + \sum_{h=1}^k \xi_{hn}\tau_{hi}\eta_{h,m} \end{pmatrix} \in \mathbb{R}^{n(m-1)}.$$

In the above notation, we take advantage of the anti-symmetric property of  $Z_{u::}$  and assume  $z_{uij} = -z_{uji}$  when  $i > j$ .



Posterior of  $\tau_j$  with  $j = 1, \dots, m$

$$\tau_j | Z, \Xi, H, T \setminus \tau_j \sim N_k^+(\Sigma_j^T (\Psi_j^T)^\top \bar{z}_j^T, \Sigma_j^T),$$

where  $(\Sigma_j^T)^{-1} = (\Psi_j^T)^\top (\Psi_j^T) + I$ ,

$$\Psi_j^T = \begin{pmatrix} \xi_{11}\eta_{11} & \xi_{21}\eta_{21} & \cdots & \xi_{k1}\eta_{k1} \\ \xi_{11}\eta_{12} & \xi_{21}\eta_{22} & \cdots & \xi_{k1}\eta_{k2} \\ \vdots & \vdots & \ddots & \vdots \\ \xi_{11}\eta_{1,j-1} & \xi_{21}\eta_{2,j-1} & \cdots & \xi_{k1}\eta_{k,j-1} \\ \xi_{11}\eta_{1,j+1} & \xi_{21}\eta_{2,j+1} & \cdots & \xi_{k1}\eta_{k,j+1} \\ \vdots & \vdots & \ddots & \vdots \\ \xi_{11}\eta_{1m} & \xi_{21}\eta_{2m} & \cdots & \xi_{k1}\eta_{km} \\ \xi_{12}\eta_{11} & \xi_{22}\eta_{21} & \cdots & \xi_{k2}\eta_{k1} \\ \vdots & \vdots & \ddots & \vdots \\ \xi_{12}\eta_{1,j-1} & \xi_{22}\eta_{2,j-1} & \cdots & \xi_{k2}\eta_{k,j-1} \\ \xi_{12}\eta_{1,j+1} & \xi_{22}\eta_{2,j+1} & \cdots & \xi_{k2}\eta_{k,j+1} \\ \vdots & \vdots & \ddots & \vdots \\ \xi_{12}\eta_{1m} & \xi_{22}\eta_{2m} & \cdots & \xi_{k2}\eta_{km} \\ \vdots & \vdots & \ddots & \vdots \\ \xi_{1n}\eta_{11} & \xi_{2n}\eta_{21} & \cdots & \xi_{kn}\eta_{k1} \\ \vdots & \vdots & \ddots & \vdots \\ \xi_{1n}\eta_{1,j-1} & \xi_{2n}\eta_{2,j-1} & \cdots & \xi_{kn}\eta_{k,j-1} \\ \xi_{1n}\eta_{1,j+1} & \xi_{2n}\eta_{2,j+1} & \cdots & \xi_{kn}\eta_{k,j+1} \\ \vdots & \vdots & \ddots & \vdots \\ \xi_{1n}\eta_{1m} & \xi_{2n}\eta_{2m} & \cdots & \xi_{kn}\eta_{km} \end{pmatrix} \in \mathbb{R}^{n(m-1) \times k},$$

and

$$\bar{z}_j^T = \begin{pmatrix} -z_{1j1} + \sum_{h=1}^k \xi_{h1}\tau_{h1}\eta_{hj} \\ -z_{1j2} + \sum_{h=1}^k \xi_{h1}\tau_{h2}\eta_{hj} \\ \vdots \\ -z_{1j,j-1} + \sum_{h=1}^k \xi_{h1}\tau_{h,j-1}\eta_{hj} \\ -z_{1j,j+1} + \sum_{h=1}^k \xi_{h1}\tau_{h,j+1}\eta_{hj} \\ \vdots \\ -z_{1jm} + \sum_{h=1}^k \xi_{h1}\tau_{hm}\eta_{hj} \\ -z_{2j1} + \sum_{h=1}^k \xi_{h2}\tau_{h1}\eta_{hj} \\ \vdots \\ -z_{2j,j-1} + \sum_{h=1}^k \xi_{h2}\tau_{h,j-1}\eta_{hj} \\ -z_{2j,j+1} + \sum_{h=1}^k \xi_{h2}\tau_{h,j+1}\eta_{hj} \\ \vdots \\ -z_{2jm} + \sum_{h=1}^k \xi_{h2}\tau_{hm}\eta_{hj} \\ \vdots \\ -z_{n,j,j-1} + \sum_{h=1}^k \xi_{hn}\tau_{h,j-1}\eta_{hj} \\ -z_{n,j,j+1} + \sum_{h=1}^k \xi_{hn}\tau_{h,j+1}\eta_{hj} \\ \vdots \\ -z_{njm} + \sum_{h=1}^k \xi_{hn}\tau_{hm}\eta_{hj} \end{pmatrix} \in \mathbb{R}^{n(m-1)}.$$

Similar to  $\bar{z}_i^T$ , we take advantage of the anti-symmetric property of  $Z_{ui}$ : and assume  $z_{uij} = -z_{uji}$  when  $i > j$ .

## B. Properties of Real World Datasets

Table 2. Properties of the three real word datasets used in Section 6

Dataset	#Users	#Items	#Ratings	Sparsity	Quantiles of #Ratings/User (min/5%/50%/95%/max)
Netflix	10,000	8,693	1,044,318	98.80%	(1/6/46/400/8,237)
Movie-Lens	6,040	3,706	1,000,209	95.53%	(20/23/96/556/2,314)
Amazon Food	10,000	29,211	162,379	99.94%	(8/8/12/36/448)

## C. Methods Considered in the Real World Application

Table 3. Specifics &amp; hyper-parameters for models used when applying to real world datasets.

Model	Parameter	Values
SAD	Implementation	In-house
	Learning Rate	[0.001, 0.002, 0.005, 0.01, 0.02, 0.05, 0.1]
	# Epochs	[2, 5, 10, 20, 50]
	$l_2$ Reg	[0.05, 0.01, 0.005, 0.001]
	$l_1$ Reg	0.01
BPR (Rendle et al., 2009)	Implementation	In-house
	Learning Rate	[0.001, 0.002, 0.005, 0.01, 0.02, 0.05, 0.1]
	# Epochs	[2, 5, 10, 20, 50]
	$l_2$ Reg	[0.05, 0.01, 0.005, 0.001]
SVD	Implementation	Surprise (package) (Hug, 2020)
	Learning Rate	[0.001, 0.002, 0.005, 0.01, 0.02, 0.05, 0.1]
	# Epochs	[2, 5, 10, 20, 50]
	Regularization	[0.05, 0.01, 0.005, 0.001]
Matrix Factorization (MF)	Implementation	Cornac (package) (Salah et al., 2020)
	Learning Rate	[0.001, 0.002, 0.005, 0.01, 0.02, 0.05, 0.1]
	# Epochs	[2, 5, 10, 20, 50]
	$\lambda$ Reg	[0.05, 0.01, 0.005, 0.001]
Probabilistic Matrix Factorization (PMF) (Mnih & Salakhutdinov, 2008)	Implementation	Cornac (package) (Salah et al., 2020)
	Learning Rate	[0.001, 0.002, 0.005, 0.01, 0.02, 0.05, 0.1]
	# Epochs	[2, 5, 10, 20, 50]
	$\lambda$ Reg	[0.05, 0.01, 0.005, 0.001]
Factorization Machine (FM) (Rendle, 2010)	Implementation	RankFM (package)
	Learning Rate	[0.001, 0.002, 0.005, 0.01, 0.02, 0.05, 0.1]
	# Epochs	[2, 5, 10, 20, 50]
	$l_2$ Reg	[0.05, 0.01, 0.005, 0.001]
Neural Collaborative Filtering (NCF) (He et al., 2017)	Implementation	MSFT recommenders (package) (Graham et al., 2019)
	Learning Rate	[0.001, 0.002, 0.005, 0.01, 0.02, 0.05, 0.1]
	# Epochs	[2, 5, 10, 20, 50]
	Batch size	[128, 256, 512, 1024]
	Network	Three layers MLP with sizes [128, 64, 32]
Variational AutoEncoder ( $\beta$ -VAE) (Liang et al., 2018)	Implementation	MSFT recommenders (package) (Graham et al., 2019)
	$\beta$ parameter	[0.001, 0.002, 0.005, 0.01, 0.02, 0.05, 0.1]
	# Epochs	[2, 5, 10, 20, 50]
	Batch size	[128, 256, 512, 1024]

## D. Real World Examples

Table 4. Examples where SAD produces a consistent prediction ( $x_{uij} > 0$  and  $p_{uij} > 0.5$ ) while BPR fails ( $x_{uij} < 0$  and  $p_{uij} < 0.5$ ).

Dataset	$u$ -th user	$i$ -th item (rating)	$j$ -th item (rating)	$x_{uij} \mid p_{uij}$			
				SAD	BPR		
Netflix	'2439493'	The Phantom of the Opera: Special Edition (4)	Crank Yankers: Season 1: Uncensored (1)	1.53	0.82	-2.80	0.06
		Lethal Weapon 4 (3)	The Jack Benny Show: Vol. 1 (2)	1.48	0.81	-1.82	0.14
		Agnes Browne (2)	Battle Arena Toshinden (1)	1.52	0.82	-0.35	0.41
		The Blues Brothers: Theatrical Cut (2)	Boris and Natasha (1)	1.49	0.82	-1.50	0.18
		Autumn in New York (5)	Sick (1)	0.87	0.70	-0.98	0.27
	'1000410'	North by Northwest (3)	Kill by Inches (1)	2.48	0.92	-0.04	0.49
		Look at Me (4)	Wonderland (1)	1.86	0.86	-0.21	0.45
		The Cruel Sea (3)	Dick Francis: The Racing Game (1)	1.85	0.86	-0.93	0.28
		A Hard Day's Night: Collector's Series (4)	The Superman Collection (Max Fleischer) (2)	1.20	0.77	-0.08	0.48
		Baby Boom (4)	House Party 2 (1)	2.47	0.92	-1.42	0.20
Movie-Lens	'00010'	Peter Pan (5)	Clerks (2)	0.70	0.67	-0.49	0.38
		White Christmas (5)	Breaking Away (3)	0.16	0.54	-0.56	0.36
		Day the Earth Stood Still (5)	To Wong Foo, Thanks for Everything! (4)	1.18	0.77	-0.74	0.32
		Peter Pan (5)	Mad Max Beyond Thunderdome (2)	0.87	0.71	-0.16	0.46
		Romeo and Juliet, 1968 (4)	Fear and Loathing in Las Vegas (2)	1.17	0.76	-0.06	0.48
	'06036'	Unbearable Lightness of Being (4)	Hope Floats (1)	1.04	0.74	-0.06	0.49
		Tender Mercies (4)	Lake Placid (1)	1.02	0.74	-0.18	0.45
		Tender Mercies (4)	Doctor Dolittle (1)	0.94	0.72	-0.26	0.43
		Farewell My Concubine (4)	Dumb & Dumber (1)	0.88	0.71	-0.41	0.40
		Velvet Goldmine (2)	Hope Floats (1)	0.27	0.57	-0.71	0.33
Amazon Food	'A100***'	Wickles Original Slices (5)	Victor M231 Ultimate Flea Trap Refills (1)	1.05	0.74	-0.86	0.30
		Natural Balance Original Ultra Reduced Calorie Dry Dog Food, Brown Rice, Chicken & Chicken Meal (3)	Vitamin Squeeze Energy Drink, Fruit Punch (1)	0.44	0.61	-1.40	0.20
		Healthy Choice New England Clam Chowder Soup (3)	Petsafe Lickety Stik Low-Calorie Liquid Dog Treat (1)	0.33	0.58	-1.51	0.18
		Red Bull Energy Drink, Total Zero (5)	Starbucks Flavored Ground Coffee, Vanilla Flavor, Velvety & Rich (3)	0.26	0.56	-1.42	0.19
		Tart Is Smart Tart Cherry Concentrate (5)	Marley Coffee, One Love Ethiopian Yirgacheffe Coffee Pods (3)	0.24	0.56	-1.54	0.18
	'AZV2***'	REESE'S Chocolate Peanut Butter Candy (5)	J & D's Baconnaisse Bacon Flavored Spread (2)	1.37	0.80	-0.75	0.32
		Bil-Jac Dog Food Dry Adult Select Formula (5)	Hormel Compleats Swedish Meatballs Microwave Tray (1)	1.21	0.77	-0.55	0.37
		MANISCHEWITZ Kluski Egg Noodles (5)	Post Honeycomb Cereal (3)	1.13	0.76	-0.45	0.39
		Martha White Muffin Baking Mix, Chocolate Chocolate Chip (5)	Good Health Kettle Style Olive Oil Potato Chips, Rosemary (3)	0.69	0.67	-0.70	0.33
		Roland Pineapple, Slices in Natural Juice (5)	Life Cereal (3)	0.49	0.62	-0.28	0.43